MECHANISMS INVOLVED IN THE FORMATION OF PHOSPHOSILICATE GLASS BY DEHYDRATION OF SPRAYED PHOSPHORIC ACID IN AN IN-LINE DIFFUSION FURNACE

Catherine Voyer, Daniel Biro, Tobias Buettner, Ralf Preu
Fraunhofer Institute for Solar Energy Systems (ISE)
Heidenhofstrasse 2, D-79110 Freiburg, Germany
phone: +49 761-4588-5246; fax: +49 761-4588-9250
email: daniel.biro@ise.fraunhofer.de

ABSTRACT: This work studies phosphosilicate glass (PSG) formation from a thin sprayed-on dopant source layer in order to increase the ability of controlling the emitter doping profile. The dopant source contains DI water, 2.5 wt% H_3PO_4 and a small quantity of surfactants. Most of the layer volume evaporates at the height of the furnace entrance. The further evolution of the dopant source layer composition is described through the dehydrative condensation of H_3PO_4 and through the reactions between the sprayed-on layer and the Si wafer. The final PSG composition is characterized by means of X-ray photoelectron spectroscopy (XPS). Furthermore, ellipsometry measurements of PSG thickness show that faster heating rates lead to thicker PSG. Finally, it is shown that a thinner dopant source layer results in a lower P surface concentration C_s and, at least in the case of fast heating rates, to a deeper emitter.
Keywords: diffusion, deposition

1 INTRODUCTION

This work reports on an in-line diffusion process that consists in in-line spraying at room temperature of a phosphorus dopant source (2.5 wt% aqueous solution of phosphoric acid H_3PO_4 with a small quantity of surfactants [1,2]) followed by phosphosilicate glass (PSG) formation and emitter diffusion in a metal-contamination-free in-line furnace [3]. Understanding PSG formation, the topic of this work, helps increasing the ability of adapting the emitter doping profile to the solar cell, in particular because the dopant source layer thickness and the resulting P source depletion are important factors in obtaining the required emitter surface concentration C_s.

2 PROCESS DESCRIPTION

A flow diagram of the emitter formation process is shown in Fig. 1. The process is carried out on polished, saw-damage etched or textured mono- or mc-Si wafers. The HNO_3/HF cleaning procedure results in a hydrophobic surface. Since the dopant source contains a surfactant mixture, the sprayed-on dilute H_3PO_4 completely wets the wafer. The drying step on the hot plate is optional. So far, no influence of this step on PSG thickness and homogeneity has been found, and it is now omitted.

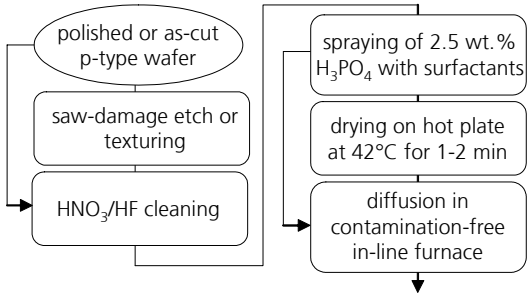

Fig. 1: Emitter formation process

2 DI WATER EVAPORATION

The dilute H_3PO_4 contains 97.5 wt% deionized (DI) water: the DI water included in commercial 85 wt% H_3PO_4 and the one used for the dilution. Practically all of the DI water evaporates at the height of the furnace entrance, or within approx. 1-2 min on the hot plate at 42°C. The time on the hot plate depends on layer thickness, and 42°C is about the maximum temperature at which the evaporation of the DI water proceeds on the hot plate without failing of the surfactant wetting action. The water evaporation can be perceived by observing the drying layer: Directly after spraying, the layer is wet and shiny. Upon drying, the layer changes its appearance. On a rough surface, it becomes mat, while on a shiny (polished) surface, it becomes coloured. On the hot plate, the layer appearance does not change anymore, even after hours. By weighing directly after spraying and after the change in appearance on the hot plate, the weight loss due to evaporation of DI water can be approximated (see Table I): it is close to 97.5%.

Table I: Weight change due to DI water evaporation

sprayer flow rate FR_{sp} (ml/min)	evaporated weight (two runs per FR_{sp}) (%)	
3.5	97.1	96.3
5	94.6	95.1

2 DEHYDRATION OF PHOSPHORIC ACID AND FINAL PSG COMPOSITION

In this section, the mechanisms of H_3PO_4 condensation by elimination of water are reviewed, and the final PSG composition is characterized.

2.1 Condensation of phosphoric acid

After evaporation of most of the DI water, the H_3PO_4 molecules and ions lie close together and tend to combine to form a variety of compounds referred to as polyphosphoric acids. The first condensation reaction describes the grouping of two H_3PO_4 molecules into a

pyrophosphoric (or diphosphoric) acid molecule $H_4P_2O_7$ by elimination of water:

$$H_3PO_4 + H_3PO_4 \rightarrow H_4P_2O_7 + H_2O.$$

The $H_4P_2O_7$ forms in turn, by further elimination of water, chain polyphosphoric acids of the form $H_{(n+2)}P_nO_{(3n+1)}$. Starting at the triphosphoric acid $H_5P_3O_{10}$, intramolecular condensation reactions can occur that produce cyclic structures (rings), as well as intermolecular reactions that produce branched structures. As the H_3PO_4 concentration increases, larger and more complex polymer molecules appear in the solution. No pure compound is ever obtained during this process, but rather a mixture of many different polyphosphoric acids of the form $H_xP_yO_z$. The proportions of the different acids in the mixture depend on the H_3PO_4 concentration, on the macroscopic state variables, such as temperature, and possibly on the system history [4]. The formal end product of the condensation is amorphous P_2O_5.

The condensation process results in a dense PSG. It was observed that the PSG does not change its appearance (a brown or blue layer) even after years of storage in normal atmosphere, or after dipping in water and drying with a nitrogen gun. The PSG is therefore not hygroscopic.

The vapour-liquid phase diagram for the H_2O-P_2O_5 system [5] shows that an azeotropic mixture with a P_2O_5 concentration of 92% is obtained at 866°C. It is therefore assumed that the sprayed-on layer has reached its minimum water content when the wafer temperature is equal to 866°C. It is not known whether complete dehydration can be reached at significantly lower temperatures.

2.2 Reaction between sprayed-on layer and silicon

Through heating, the dopant source layer also reacts with the Si wafer. Phosphorus and oxygen diffuse down to the Si surface, to then diffuse into the wafer and be incorporated in the crystal lattice. Furthermore, Si diffuses up into the dopant source layer, whereby mixed compounds with Si, P and O are produced. Oxygen is also available from the ambient air for diffusion into the dopant source layer.

Silicon reacts with the phosphorus compounds (cross-linked or linear polymer molecules) in the dopant source layer according to the general chemical equation:

$$H_aP_bO_c + d\ Si(s) \rightarrow Si_wP_x(s) + Si_yO_z(s)$$

where the Si-P and Si-O bonds can be situated in the dopant source layer as well as in the Si lattice.

In addition, Si can react with water from the dopant source layer or with oxygen from the ambient air according to the well-known equations of wet or dry oxidation:

$$Si(s) + 2\ H_2O(l) \rightarrow SiO_2(s) + 2H_2(g)\uparrow$$
$$Si(s) + 2\ O_2(g) \rightarrow SiO_2(s)$$

2.3 Final PSG composition

The PSG chemical composition was analyzed by means of X-ray photoelectron spectroscopy (XPS). An overview spectrum first showed the presence of P, Si, O and C at the sample surface. The sample was then sputtered with argon ions and the atomic concentration of P, Si, O and C was measured once per minute. The 10×10 mm² sample was cut from a FZ-Si wafer with a chemically polished surface and a resistivity ρ of 3.2-4.8 Ω-cm. The sample after XPS analysis is shown in Fig. 2 (ellipsometry) and Fig. 3 (surface profilometry). The PSG thickness around the measurement area was also measured using ellipsometry before the XPS analysis and is equal to exactly 100 nm. The PSG thickness measurement is not valid in the cavity region, where the bare Si is exposed. Using surface profilometry, a cavity depth of 130 nm was approximated: 100 nm in the PSG and 30 nm in the Si.

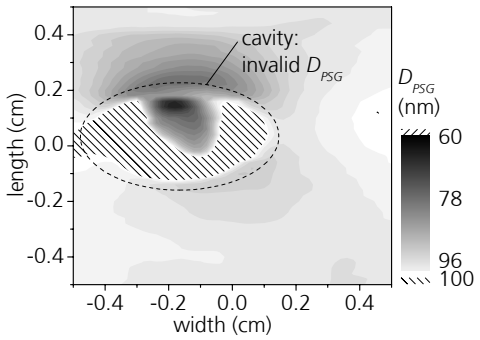

Fig. 2: Ellipsometry of PSG thickness D_{PSG} after XPS analysis

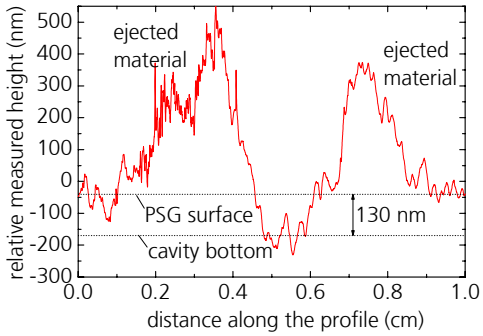

Fig. 3: Surface profilometry after XPS analysis

The XPS profiles are shown in Fig. 4. Since the carbon content stays under 5%, it can be attributed to the measurement error. It is therefore assumed that the final PSG does not contain any surfactant residuals, i.e. that the surfactants burn out during PSG formation.

The oxygen content vanishes at about the 33rd from 42 measurement points. Approximating the PSG/Si interface to this depth, a PSG thickness-to-cavity depth ratio of 0.79 (= 33/42) is calculated. This agrees with the ellipsometry and profilometry measurements, which resulted in an approximated ratio of 0.77 (= 100/130).

Across a depth of about 35 nm underneath the PSG surface, a compound ratio between SiO_2 and P_2O_5 can be calculated from the atomic ratios between P, Si and O. For example, at the 6th measurement point, the atomic P, Si, O and C concentrations are equal to 2.8%, 30.8%, 66.4% and 0% respectively. This corresponds to 90% SiO_2 and 10% P_2O_5.

Starting at a depth of about 35 nm, the O concentration follows a typical exponential diffusion curve. It is assumed that O diffuses into the wafer. In the first 35 nm, the O content stays approx. constant despite the losses to the Si bulk. This is possibly due to an O replenishment of the upper dopant source layer region from the ambient air. The PSG/Si interface is shown at

the approximate location where the O concentration reaches zero, i.e. at the 33rd measurement point of 42.

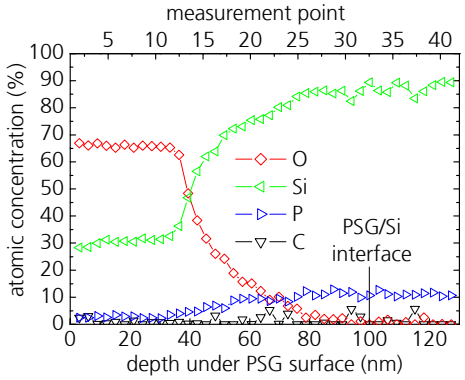

Fig. 4: XPS profiles for the elements P, Si, O and C

The P-to-Si ratio around the PSG/Si interface agrees with the surface concentration of the doping profile measured using secondary ion mass spectrometry (SIMS): this is the profile "*a*" in Fig. 9. Extrapolating across the concentration decrease close to the surface typical to SIMS profiles, the P surface concentration of the SIMS profile C_s is equal to 5×10^{20} atoms/cm^3. Since the Si lattice contains 5×10^{21} atoms/cm^3, the P-to-Si ratio is equal to 10%, like in Fig. 4.

3 INFLUENCE OF HEATING RATE ON PSG THICKNESS

Through heating, the sprayed-on layer turns into a dense PSG. Higher heating rates lead to thicker PSG. During H_3PO_4 condensation, not only water but also P_2O_5 evaporates. It appears that a faster condensation leads to less P_2O_5 evaporation and therefore to a thicker PSG.

A first example in shown in Fig. 5. The six polished 125×125 mm^2 wafers were spray-coated, shortly dried on the hot plate at 42°C and heated in a rapid thermal processing (RTP) furnace up to 900°C. The RTP heating time lasted in total 170 s, from which the temperature ramp-up from 100°C to 900°C took 90, 70 or 50 s. Fig. 4 shows the average PSG thickness D_{PSG} on each wafer.

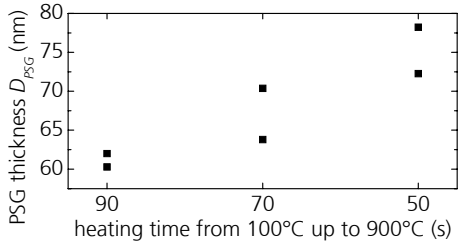

Fig. 5: Thicker PSG through faster temperature ramp-up in a single-wafer RTP furnace

Fig. 6 shows another example for 25 combinations of plateau temperature T_p and transport speed V in the in-line furnace. Each point corresponds to the average D_{PSG} on one saw-damage etched 125×125 mm^2 Cz-Si wafer. (The employed ellipsometer can also measure D_{PSG} on this surface structure.) A faster PSG formation, due to a higher heating rate in the furnace entrance area or to a higher plateau temperature, leads to thicker PSG. An increase in D_{PSG} is observed up to about V = 150 mm/min, followed by a stabilization and a further increase up to V = 600 mm/min. The higher D_{PSG} at higher T_p must be due to a faster temperature ramp-up and/or to a faster final PSG densification at the beginning of the temperature plateau.

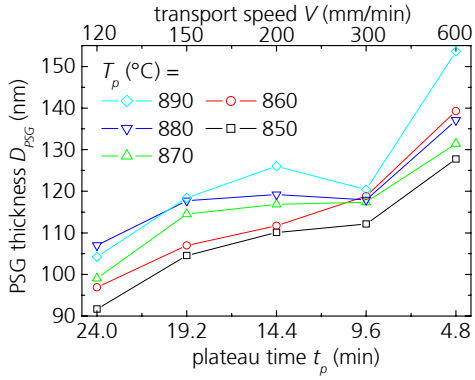

Fig. 6: Thicker PSG through higher V or T_p in the in-line diffusion furnace

4 RELATION BETWEEN DOPANT SOURCE LAYER THICKNESS AND DOPING PROFILE

An important parameter of the emitter formation process is the dopant source layer thickness. A common practice when using sol-gel ("spin-on dopant": phosphosilicate polymer molecules dissolved in organic solvent) is to coat the wafer with a sufficiently thick layer in order to obtain a practically inexhaustible dopant source. It this way, it is possible to minimize the dependence of sheet resistance R_{sh} on dopant source layer thickness. However, this practice is for two reasons hardly compatible with the use of dilute H_3PO_4 as the dopant source:

1. In order to minimize electron-hole pair recombination, the emitter profile needs a sufficiently low surface concentration C_s. The resulting C_s depends on the diffusion temperature-time curve as well as on the dopant source layer concentration and thickness. Since the condensation of the sprayed-on phosphoric acid results in a highly concentrated dopant source, a thick sprayed-on layer can result in too high a C_s. In order to obtain a sufficiently low C_s at high temperatures close to 900°C (which allow for a sufficiently short diffusion time), the diffusion must proceed from a thin and, hence, finite dopant source.

2. In in-line furnaces, the wafers are heated relatively fast. The phosphoric acid condensation may therefore not be completed until the wafer reaches high temperatures at which a significant P diffusion in Si already started. Since the required time for complete PSG densification depends on dopant source layer thickness, R_{sh} can also depend on layer thickness.

For these two reasons, a dependence of R_{sh} on D_{PSG} is practically unavoidable. This means first that a sufficiently homogeneous D_{PSG} is required and second that D_{PSG} is an important parameter in obtaining the required C_s.

Fig. 7 shows a R_{sh} map for plateau temperatures T_p from 850°C to 890°C, plateau times t_p from 4.8 to 24 min and two flow rates of the dopant source to the sprayer nozzle FR_{sp}, 3.5 ml/min and 5 ml/min. Each point shows R_{sh} averaged over one 125×125 mm^2 textured Cz-Si

wafer with a resistivity ρ of 0.5-1.7 Ω-cm. Since each point only corresponds to a single wafer, the results differ from the one expected when averaging over many wafers. The quadratic polynomial regression in Fig. 8 allows for smoothing of the experimental data.

At the highest V (left side of the graph), the lower FR_{sp} led to lower R_{sh}, while at the lowest V, the situation is opposite: the higher FR_{sp} led to lower R_{sh}. This latter case is the intuitively expected one: A thicker dopant source layer results in more diffusion. The first case is however more surprising. The most probable explanation is that thicker layers require a longer PSG densification, and this results in a weaker diffusion in the first heating zones of the furnace. It is assumed that a thicker dopant source layer leads in all cases to a higher C_s. The higher R_{sh} obtained from thicker dopant source layers is therefore due to a lower P concentration in the deeper layers of the emitter. An example is shown in Fig. 9. The higher FR_{sp} (5 ml/min) led to a higher C_s. The P concentration is only higher in the first 500 nm, where a big portion of the P is electrically inactive and therefore does not contribute to the reduction of R_{sh}. Starting at a depth of about 0.2 µm, the P concentration of profile *b* is clearly below the one of profile *a*. In this case (T_p = 880°C, t_p = 16.8 min), both FR_{sp} result in almost equal R_{sh}.

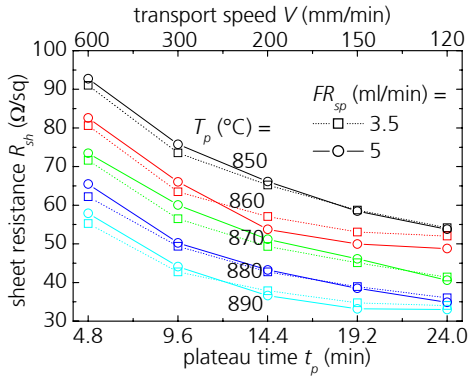

Fig. 7: R_{sh} map

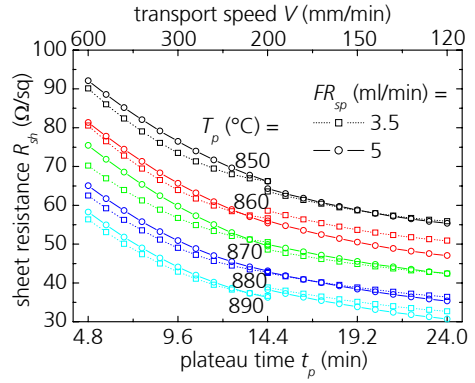

Fig. 8: R_{sh} map, quadratic polynomial regression

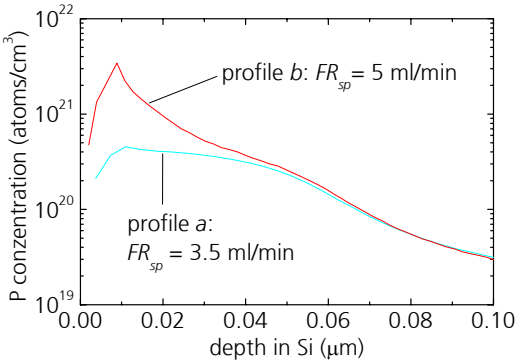

Fig. 9: SIMS profiles for T_p = 880°C and t_p = 16.8 min

5 CONCLUSION

Mechanisms involved in the formation of PSG from a sprayed-on layer of dilute phosphoric acid in an in-line diffusion furnace were examined. Since the DI water, which composes most of the sprayed-on layer, evaporates at the height of the furnace entrance, PSG formation involves primarily the dehydrative condensation of the H_3PO_4 and the reactions between dopant source and Si. The XPS analysis of the final PSG composition showed the diffusion of P in Si and the resulting P depletion at the PSG surface. Through the dopant source layer thickness and, hence, degree of P depletion, the emitter surface concentration C_s can be adjusted. The dopant source layer thickness depends in turn on sprayer flow rate and heating rate. Understanding these interactions allows for a flexible control of the emitter profile.

6 ACKNOWLEDGEMENTS

The authors thank A. Hartel for in-line diffusion, D. Mössner for XPS analysis and K. Mayer for helping with the chemical explanations. This work has been partially supported by the European Union (SES6-CT-2003-502583, Crystal Clear). C. Voyer received a scholarship from the German Academic Exchange Service (DAAD).

7 REFERENCES

[1] C. Voyer, D. Biro, K. Wagner, J. Benick, R. Preu, J. Koriath, M. Heintze and H.M. Wanka, Proceedings of the 20th European Photovoltaic Solar Energy Conference, Barcelona, Spain (2005) 1415.

[2] D. Biro, C. Voyer, H. Wanka et al., German Patent 102005025933.

[3] D. Biro, G. Emanuel, R. Preu and G. Willeke, From PV Technology to Energy Solutions, Rome, Italy (2002) 303.

[4] A.-L. Huhti and G.P. A., Canadian Journal of Chemistry 34 (1956) 785.

[5] H. Bitterer, G. Czack, G. Kirschstein, A. Kunze, H. Lehl, G. Pietsch-Wilcke, L. Thaler and E. Ühlein, Gmelins handbuch der anorganischen chemie, Vol. 16, Verlag Chemie GmbH, Weinheim/Bergstr., 1965.